In-situ handheld 3D Bioprinting for cartilage regeneration

Running title

In vivo study in a sheep full thickness chondral defect. Early results.

Claudia Di Bella [1,2], Serena Duchi [1], Cathal D. O'Connell [3], Romane Blanchard [1], Cheryl Augustine [1], Zhilian Yue [3], Fletcher Thompson [3], Christopher Richards [3], Stephen Beirne [3], Carmine Onofrillo [1,3], Sebastien H. Bauquier [4], Stewart D. Ryan [4], Peter Pivonka [1], Gordon G. Wallace [3], Peter F. Choong [1,2].

1. Department of Surgery, University of Melbourne
2. Orthopaedic Department, St Vincent's Hospital, Melbourne
3. ARC Centre of Excellence for Electromaterial Science, Intelligent Polymer Research Institute, University of Wollongong
4. Translational Research and Animal Clinical Trial Study Group (TRACTS) Faculty of Veterinary and Agricultural Sciences, University of Melbourne

Corresponding Author:

Claudia Di Bella, MD PhD FRACS

Department of Surgery, St Vincent's Hospital Campus

University of Melbourne

29 Regent St, Fitzroy

Author Manuscript

This is the author manuscript accepted for publication and has undergone full peer review but has not been through the copyediting, typesetting, pagination and proofreading process, which may lead to differences between this version and the Version of Record. Please cite this article as doi: 10.1002/term.2476

This article is protected by copyright. All rights reserved.

VIC 3065, Australia

Claudia.dibella@unimelb.edu.au

Author Manuscript

This article is protected by copyright. All rights reserved.

Abstract

Articular cartilage injuries experienced at an early age can lead to the development of osteoarthritis later in life. In situ 3D printing is an exciting and innovative bio-fabrication technology that enables the surgeon to deliver tissue-engineering techniques at the time and location of need. We have created a hand-held 3D printing device (Biopen) that allows the simultaneous co-axial extrusion of bioscaffold and cultured cells directly into the cartilage defect in vivo in a single session surgery. This pilot study assesses the ability of the Biopen to repair a full thickness chondral defect and the early outcomes in cartilage regeneration, and compares these results to other treatments in a large animal model.

A standardised critical-sized full thickness chondral defect was created in the weight-bearing surface of the lateral and medial condyles of both femurs of 6 sheep. Each defect was treated with one of the following treatments: (i) hand-held in situ 3D printed bioscaffold using the Biopen (HH group), (ii) pre-constructed bench-based printed bioscaffolds (BB group), (iii) micro-fractures (MF group) or (iv) untreated (Control, C group). At 8 weeks after surgery, macroscopic, microscopic and biomechanical tests were performed.

Surgical 3D bio-printing was performed in all animals without any intra- or post-operative complication. The HH Biopen allowed early cartilage regeneration.

This article is protected by copyright. All rights reserved.

Results of this study show that real-time, in vivo bioprinting with cells and scaffold is a feasible means of delivering a regenerative medicine strategy in a large animal model to regenerate articular cartilage.

Keywords

3D Bioprinting, cartilage regeneration, Bioscaffold, In vivo large animal study, Tissue Engineering, surgical 3D printer

Author Manuscript

This article is protected by copyright. All rights reserved.

1. Introduction

Joint injuries cause substantial pain and loss of function, and may result in osteoarthritis (OA) at considerable cost to the patient and the healthcare system. Current surgical procedures, such as microfracture, mosaicplasty and osteochondral allografts have limited "effectiveness"(Lewis et al., 2006, Tetteh et al., 2012) and no treatment stands out as significantly better than another(Farr et al., 2011). Failure occurs because of two reasons: (i) Healing cartilage forms fibrocartilage, which is unable to sustain the shear and compressive forces that characterise normal articular hyaline cartilage. (ii) Poor integration of graft with host cartilage results in breakdown of tissue at the graft/host junction(Gilbert, 1998, Khan et al., 2008).

Bioprinting, defined as the simultaneous deposition of structural biomaterials and living cells, is emerging as an important tissue engineering strategy to recreate the microphysical environment and the relationship between cells, their matrix and local anatomy (Gao and Cui, 2016, Chung, 2013). Current 3D printing technology is characterised by the production of a scaffold in the laboratory that is subsequently shaped to match the surgical defect; in some cases, "custom made" scaffolds are created using CT and/or MRI images of the defect as templates (Kang et al., 2016). Although this technique potentially creates a matching scaffold geometry for the injury that needs repair, the resolution of CT and MRI scans places an upper limit on the achievable fit. Furthermore, the necessary surgical debridement before scaffold implantation make a "perfect

This article is protected by copyright. All rights reserved.

match" technically unachievable. These two reasons explain the inevitable graft/host mismatch of pre-constructed scaffolds, which in turn is one of the reasons that might impede good integration of the scaffold (Cui et al., 2012). Based on the drawbacks of this technology, we have developed and evaluated a novel alternative based on in-situ 3D bioprinting using a hand-held bioprinter, called the "Biopen"(O'Connell, 2016). This device, which is deployed during surgery, bypasses the need for prior biofabrication of a chondral implant in the laboratory.

The Biopen has a number of advantages over robotically manipulated bench based 3D printers in particular with respect to surgical procedures involved in cartilage repair: (a) being a manually operated tool it allows for surgical sculpting of the substitute tissue to achieve the desired structure, (b) increased surgical dexterity allows for deposition within crevices or beneath overhangs in native tissue, (c) as a smaller, less cumbersome device it can be easily brought in/out of the surgical field, (d) it is easier to sterilise and keep sterile and (e) the flexibility of *in situ* biofabrication allows for freeform construction of substitute tissue at the surgeon's discretion, with the possibility of creating multiple layers specifically designed for different tissues (i.e. bone and cartilage).

The purpose of this pilot study was to establish the surgical applicability of this tool for the regeneration of full thickness chondral defects in the pre-clinical setting, using the large animal ovine model.

Author Manuscript

This article is protected by copyright. All rights reserved.

Author Manuscript

This article is protected by copyright. All rights reserved.

2. Materials and Methods

2.1 BIOPEN DESIGN

We have engineered a hand-held biofabrication tool (Biopen), which enables the deposition of living cells and biomaterials (Bioscaffold) in a manual, direct-write fashion. This system integrates scaffold (Bioink) chambers, a multi-inlet extruder nozzle, a light source to catalyse phase transformation of the ink, and a motorised extrusion system (Fig 1A-D) (O'Connell, 2016). The nozzle has a specific internal structure that allows the extrusion of Bioink in a core/shell distribution, so that the extrusion of Bioink comprising living cells occurs within an inner core protected by a more robust biomaterial around it (Fig 1C). The "core" is constituted by Bioink laden with stem cells, while the "shell" is Bioink mixed with photoinitiator to allow photo-curing (hardening) of the Bioscaffold during printing. This specific distribution permits the creation of multiple layers of Bioscaffold during the printing process (Fig 1D).

2.2 PREPARATION OF STEM CELLS

Mesenchymal Stem Cells (MSC) were collected and prepared using an adaptation of our previously published protocol (Ye et al., 2014). Briefly, the infra-patellar fat pad of a recently euthanized sheep was collected, washed, cleaned of fibrous material, finely diced and digested with 0.2% Collagenase Type 1 for three hours at 37^0C under constant agitation. The released cells were filtered and

Author Manuscript

This article is protected by copyright. All rights reserved.

centrifuged. The supernatant was discarded and the cell pellet re-suspended in Red Cell Lysis Buffer and incubated at room temperature for 10 minutes. This was then filtered and centrifuged one more time, the cells re-suspended in PBS, counted and plated in monolayer culture (75 cm^2 tissue culture flask) at 5,000 cells/cm^2 in stromal media containing DMEM supplemented with 10% FBS, 1× antibiotic/antimycotic solution, 1× Glutamax, and 15 mM HEPES. Cells were expanded to passage 3 and then frozen at -80^0C , ready to be added to the Bioink at a concentration of 2.5x10^6/ml.

2.3 BIOSCAFFOLD

The bioink, HA-GelMa, is composed of gelatin methacrylamide (GelMa) and hyaluronic acid methacrylate (HAMA) hydrogel, which is known to have excellent performance in cartilage regeneration (Schuurman et al., 2013) (Fedorovich et al., 2012, Jeong and Atala, 2015). Our published protocol was used to prepare the HA-GelMa bioink (O'Connell, 2016). Briefly, 100 mg/mL GelMa and 20 mg/mL HAMA are dissolved in sterile DPBS (Lonza) containing 100U/mL penicillin and 100 μg/mL of streptomycin (Gibco) to give a final concentration of 10% wt GelMa and 2% wt HAMa.

The Bioscaffold in this study comprises HA-GelMa Bioink + allogeneic adipose-derived Mesenchymal Stem Cells (MSCs), which is printed as the *core*, and HA-GelMa Bioink + photoinitiator, which is printed as the *shell*.

Author Manuscript

This article is protected by copyright. All rights reserved.

For the *core*, MSCs are added to HA-GelMA (without photoinitiator) at room temperature at a concentration of $2.5x10^6$/mL; the gel is gently stirred to allow uniform distribution of the cells, and then transferred to a printing cartridge (3cc syringe barrel, EFD) and put in ice for 10 minutes, to allow the mixture to reach a temperature of approximately 4^oC. This temperature engenders physical crosslinking of the hydrogel, increasing bioink viscosity and improving control of the printed pattern.

For the *shell* component of the Bioink, the photoinitiator VA-086 (2,2'-Azobis[2-methyl-N-(2 hydroxyethyl)propionamide], Wako Pure Chemical Industries Ltd, is dissolved at 10 wt% in sterile DPBS solution and then added to the HA-GelMa. The final formulation is 10 wt% GelMa, 2 wt% HAMA and 0.5 wt% VA-0860. The shell Bioink is transferred to a printing cartridge and then stored at 4^oC covered in foil.

The Biopen is loaded with two cartridges of Bioink; one for the core and one for the shell, under sterile conditions immediately before the surgical application. Sterility of the ink cartridges and the extrusion nozzle is achieved through nominal surgical procedures of autoclaving and sterile packaging.

Following surgical printing, the Bioscaffold was exposed to 365 nm light using an Omnicrue LX400 LED light source fitted with a 12 mm lens, at an intensity of 130 mW/cm^2 for 60s to photocrosslink the methacrylated hydrogels. We have previously demonstrated that the cell viability of mesenchymal stem cells encapsulated under these conditions is very high (97%) (O'Connell, 2016).

This article is protected by copyright. All rights reserved.

Author Manuscript

2.4 STUDY DESIGN

Use of all animals and procedures in this study was approved by the University of Melbourne Animal Ethics Committee [ID 1513586]. Six mature, male Merino cross sheep, aged 2-3 years old, with body weights between 60 and 87 kg (mean 69kg) were used. In each sheep, bilateral medial arthrotomy of the stifle (knee) joint was performed to expose the distal femoral condyles. An 8 mm critical-sized, full-thickness chondral defect was created in each condyle resulting in a total of 4 defects per sheep (Fig 2a). Each defect was treated with either: (i) Hand-Held in situ 3D printed Bioscaffold using the Biopen (HH group), (ii) pre-constructed Bench-Based printed Bioscaffolds (BB group), (iii) Micro-fractures (Clinical Control, MF group) or (iv) left untreated (Negative Control, C group). Each sheep received all treatment groups. A computer generated block randomisation of 6 sets of 4 unique numbers per set (https://www.randomizer.org/) was performed to determine treatment group allocation of each defect to avoid location bias.

Sheep were allowed to fully weight bear after surgery. Sheep were euthanized 8 weeks after surgery and the femoral condyles collected for analysis.

2.5 SURGICAL PROCEDURE

Author Manuscript

This article is protected by copyright. All rights reserved.

Sheep were premedicated with IV diazepam (0.5 mg/kg). General anaesthesia was then induced with IV administration of thiopental to effect (5 - 10mg/kg) and the trachea of the sheep was intubated with a cuffed endotracheal tube. Anaesthesia was maintained with isoflurane (1 – 2 %) in oxygen. Perioperative analgesia consisted of IV hydromorphine (0.1 mg/kg) and epidural morphine (0.1 mg/kg). Antimicrobial prophylaxis (cephalexin, 10 mg/kg) was provided. Postoperative analgesia consisted of transdermal fentanyl patches (two 50 mcg/hr, one on each hindlimb) and carprophen (2mg/kg per os twice daily for 6 days).

The stifle (knee) joints were clipped of wool and prepared for aseptic surgery. Sheep were positioned in dorsal recumbency to allow access to both hindlegs. Medial parapatellar arthrotomies were performed in both hindlegs and the lateral and medial femoral condyles exposed. An 8-mm circular critical sized full thickness chondral defect was created in the weight-bearing surface of the lateral and medial condyles of both femurs using a dermal skin biopsy punch and a Volkman curette. Care was taken to ensure that the defect was limited to the cartilage layer only, preserving the subchondral bone. Each defect was treated with one of four treatments based on the random assignment:

- *HH group (Fig 2 b)*: the two Bioinks (core and shell) were prepared on the same day of the surgical procedure, put in cartridges in the fridge at 4^0C and, following sterile procedures, inserted in the Biopen immediately

Author Manuscript

This article is protected by copyright. All rights reserved.

before in-vivo 3D printing. The in-vivo Bioscaffold 3D printing was performed directly in the chondral defect.

- *BB group*: One week before the surgical procedure, the HA-GelMa Bioscaffold was extruded in a non-coaxial technique using a table-top bioprinter (Bioplotter, Invisiontec) in a 1 x 1 x 0.1 cm block in a petri dish. MSCs were added to the bioscaffold at a concentration of $2.5x10^6$/ml. The bioscaffold was then immersed in stromal media (DMEM-High Glucose, 1% FBS, 1% ITS, 100 nM dexamethasone, 50 µg/mL ascorbic acid, antibiotic/antimycotic) and incubated at 37 ^oC, to allow cell adhesion to the gel. During the surgical procedure, an 8 mm diameter cylinder was cored out of the bioscaffold block and inserted in the defect.
- *Clinical group*: 5 holes were created in the defect area using a 1.0 mm microfracture awl and confirmed by bleeding bone.
- *Control group*: the defect was left untreated.

In both the BB and HH groups, a thin layer of fibrin glue (Tisseel, Baxter) was sprayed on top of the bioscaffold to prevent its mobilization from the defect (Fig 2c).

Sheep were housed in an indoor group pen and were allowed to fully bear weight after surgery. Sheep were euthanized by intravenous administration of pentobarbitone 88 mg/kg) 8 weeks after surgery. Stifle joints were opened and disarticulated and the femoral condyles retrieved for analysis.

Author Manuscript

This article is protected by copyright. All rights reserved.

2.4 MACROSCOPIC, MICROSCOPIC AND BIOMECHANICAL EVALUATION

Macroscopic Evaluation: Femoral condyles were explanted and photographed; the defects were macroscopically assessed using the ICRS cartilage repair assessment protocol (Table 1) (Brittberg and Winalski, 2003) by two independent investigators in a blinded fashion.

Osteochondral blocks with the repaired defect in the centre and host bone-cartilage margin of at least 10 mm in the periphery were then collected using a high precision bone saw (Buehler Isomet1000 Precision Sectioning saw). The block was then bisected in the coronal plane to allow biomechanical and biochemical analysis (Fig 2d). One half was used fresh for biomechanical compression testing (indentation test) using the TA ElectroForce5500 mechanical loading device (Bose), while the other half was processed for histological analysis. The bisection was performed in a standardised fashion in all specimens to obtain unbiased biomechanical and histological analysis.

Biomechanical Evaluation: The bottom of the retrieved osteochondral block was horizontally cut to ensure that the half condyle sat flat on the culture dish and that the tip of the indenter was directed orthogonally to penetrate the surface of the defect (Figure 5a). Samples were kept hydrated by being immersed in PBS solution during the entire testing duration. The tests were performed at room temperature using the TA ElectroForce5500 mechanical loading device (Bose) fitted with a calibrated 5 lbf load cell and a custom-made stainless steel, cylindrical indenter (diameter =1 mm). We employed a three-stage stress

This article is protected by copyright. All rights reserved.

relaxation indentation protocol, which allows calculation of the instant and equilibrium compression modulus of cartilage together with typical peak stress and relaxation times (Stok et al., 2010, Korhonen et al., 2002). Load, displacement, and time are measured from the tests, and subsequently converted into stress and strain data using the information about indenter area and sample thickness. A LOWESS smoothing algorithm is applied to the data before analysis. These parameters were performed for all study groups and compared to undamaged hyaline cartilage (host cartilage).

Microscopic Analysis: The remaining half of the osteochondral block was fixed in 10% formalin, decalcified and processed for routine histological and immunohistochemical evaluation and scored using a modified O'Driscoll scoring (Table 2), according to the OARSI recommendations (Rutgers et al., 2010). Immunohistochemistry was performed to assess the expression of collagen I and collagen II, as markers of fibrocartilage and hyaline cartilage respectively.

2.5 STATISTICAL ANALYSIS

Data were analysed with the Friedman test, to test for differences between all four groups. Subsequently, the Wilcoxon signed-ranked test was performed to test for parameter differences between each pairwise group comparison. Significance cut-off was set at $p<0.05$. Data was analysed using Stata version 14 (StataCorp, College Station, Texas).

Author Manuscript

This article is protected by copyright. All rights reserved.

Results

1) SURGICAL 3D BIOPRINTING

The Biopen was used as a surgical tool in all cases without any intra-operative or post-operative complications. In particular the use of the Biopen was not associated with any infection. Technically, the Biopen was considered very practical and operator friendly by the two surgeons involved in the operations. The Biopen could be hand held in a similar way as other surgical instruments and did not require changes in technical practice nor any specific training. The surgeon could control the thickness of the 3D printed material, its shape and the speed of printing; the supporting un-scrubbed team could adjust these parameters at any time, based on surgeons' preferences. In all cases the Biopen delivered a 3D printed Bioscaffold that perfectly fitted the defect in terms of shape and depth (Fig 2c).

2) POST OPERATIVE IN VIVO OUTCOMES

All animals survived the 8 week in vivo period. Bilateral stifle surgeries were well tolerated in all animals. Additional analgesia beyond five days was provided in two animals for an additional 3 days.

3) MACROSCOPIC ASSESSMENT

In all cases, at arthrotomy, no clinical signs of inflammation or infection were observed. The defect was clearly visible in all groups (Fig 3a). The vast majority of the defects, regardless of their treatment, obtained Grade IV score (severely

Author Manuscript

This article is protected by copyright. All rights reserved.

abnormal, 0-3), however in the HH group, 1 defect scored in the Grade II (nearly normal, score 8) and one in the Grade III (abnormal, score 6). In the BB group, all defects obtained a Grade IV score, while in both the MF and in the C groups, one defect scored in the Grade III (score 5 and 6 respectively).

There was better overall macroscopic appearance in the HH group compared to all other groups, statistically significant versus MF ($p=0.0269$) and BB groups ($p=0.0277$), and very close to significance versus C group ($p=0.0578$). The BB group scored similarly to the MF group, while the C group showed a better macroscopic appearance when compared to the BB ($p=0.034$) but not to the MF group ($p=0.275$) (Fig 3b).

4) HISTOLOGY AND IMMUNOHISTOCHEMISTRY

Histologic assessment of repair was consistent with the macroscopic findings, however there was no statistically significant difference when all groups where compared ($p=0.2287$). At this early time point, there was minimal evidence of repair/regeneration in all groups, as depicted by the low scoring obtained in all the samples. Despite variability within each group, overall the HH group showed a higher amount of newly regenerated cartilage with evidence of chondrocytes columnar alignment, and absence of subchondral bone deformation or collapse, however there was minimal lateral integration. The surface in the vast majority of the cases appeared with slight to moderate fibrillation. On the other hand, all the other groups showed variable amount of regenerated cartilage characterised

Author Manuscript

This article is protected by copyright. All rights reserved.

by severe fibrillation or disruption of the surface; also de-arrangement of subchondral bone, including subchondral cysts and collapse was noted, and was more evident in the microfractures group. In all groups, there was absence of bonding to adjacent cartilage. The HH Group showed a similar Safranin O staining compared to the other groups. Collagen II immunohistochemistry staining showed that new tissue formation within the defect was mainly made of hyaline cartilage, with the exception of the MF group, in which fibrocartilage was evident in the defect area (Fig 4a).

The HH group showed a significantly higher O'Driscoll score when compared to the MF Group ($p=0.0350$) but not to the other groups. Similarly, the C group scored significantly better than the MF group ($p=0.0330$) (Fig 4b).

5) BIOMECHANICAL TESTS

Specimen thickness and biomechanical data are summarised in Figure 5b-e. The mean thickness measured for different intervention strategies and the host cartilage ranged between 0.7 mm and 1.0 mm with quite large standard deviation (SD) (Fig 5a). The instantaneous Young's modulus for HH and BB groups were similar around 0.5 MPa and slightly lower than the host cartilage of 0.6 MPa. On the other hand, the Young's modulus of MF and C groups were generally lower than HH, BB and host cartilage. Standard deviation for all samples was quite large and sample size low, consequently care needs to be

Author Manuscript

This article is protected by copyright. All rights reserved.

taken with interpretation of data (Fig 5b), and no statistically significant differences were detected.

The equilibrium modulus of HH, BB and control groups were similar, being around 6 MPa. This differed from the MF group, where the mean equilibrium modulus was around 10 MPa. The equilibrium modulus of host cartilage is around 5 MPa (Fig 5c).

The maximum stress obtained at 30% deformation was around 0.17 MPa for HH and BB groups, while for host cartilage it was around 0.14 MPa (Figure 5d).

Author Manuscript

This article is protected by copyright. All rights reserved.

Discussion

Attempts with the use of biphasic and multiphasic scaffolds are very promising in regenerating the osteochondral unit, however difficulties in the lateral and basal integration still remain (Hunziker, 2002). Furthermore, pre-constructed scaffolds, similar to autologous osteochondral grafting, cannot perfectly recapitulate the correct radius of curvature of the defect that needs to be repaired. This mismatch between graft and host has been reported as one of the possible reasons for the unsatisfactory results of these techniques (Jakob et al., 2002, Balint et al., 2005, Tognana et al., 2005, Khan et al., 2008).

The Biopen is an innovative solution to deliver in situ 3D printing technology for tissue engineering approaches as it allows independent extrusion conditions for each chamber, which enables geometric control of the printed structure, and the creation of compositional gradients, i.e., functionally graded materials. This permits the delivery of different layers and cell types, making it ideally placed to tackle cyto-matrical variations often found in complex tissues such as cartilage. A further innovative aspect is that the Biopen can be manually operated during surgical procedures, thus harnessing the surgeon's dexterity to create a bespoke construct avoiding the step of the biofabrication in laboratory. In this study we have demonstrated that the Biopen can be used to repair a full thickness chondral defect in a preclinical large animal model.

The first key finding is that we have succeeded in applying the Biopen in a surgical setting without peri-operative complications. A crucial question over the

Author Manuscript

This article is protected by copyright. All rights reserved.

introduction of biofabrication technologies into theatre is the demonstration of robust sterilisation protocols, because 3D bioprinters are typically bulky pieces of equipment housed in stand-alone biosafety cabinets. The compact design of the Biopen simplifies this issue, and the device can be sterilised using similar methodologies used for other manual tools in orthopaedics. In addition, the components of the Biopen directly exposed to cells (the ink cartridges, extrusion pistons, and extrusion nozzle) can be removed for separate sterilisation by autoclave. These steps minimise the risk of complications, without departing from nominal surgical procedures.

The second key finding is the demonstrated ease of use of the Biopen in a mock clinical situation. Eight successful Biopen procedures were performed without the need for specific training of either the surgeons or the supporting team. To reduce any barriers to translation, the Biopen has been ergonomically designed to closely resemble typical surgical tooling.

The third key finding is our demonstration of early promise in the clinical efficacy of the Biopen strategy. According to blinded ICRS and O'Driscoll scoring, in-vivo 3D printed bioscaffold showed better overall macroscopic and microscopic characteristics when compared to pre-constructed 3D Bioscaffolds, microfractures and untreated controls. Importantly, histology and immunohostochemistry analysis showed early formation of hyaline-like cartilage with restoration of columnar chondrocyte distribution, and maintenance of the subchondral bone integrity. Lateral integration remained an issue possibly due

Author Manuscript

This article is protected by copyright. All rights reserved.

to the early time point analysis, however further work is necessary to achieve immediate bonding between the bioscaffold and the host cartilage. We believe that a chemical modification of the biomaterial, which allows its immediate adhesion to the host tissue, would greatly improve lateral integration by guaranteeing immediate graft-host adhesion. This would also maintain the correct position of the scaffold after its application (Sharma et al., 2013). Interestingly, the control group scored better histologically when compared to the MF and BB groups. Despite the lack of regenerated cartilage, the control group showed subchondral bone integrity, which explains the relatively high score. No significant biomechanical differences in condyle explants were detected between the four treatment groups, which may be a function of the short study duration. The variability of the quality of the regenerated cartilage within the defects in all groups limited the significance of our biomechanical data, due to the necessity to bisect the specimen. However, the standardisation of the level of bisection allowed us to obtain data that reliably reflected the mechanical performance of the regenerated tissue.

This study has several limitations. Firstly, it is a pilot study limited to 8 weeks, which therefore has limited power in detecting differences between groups and has minimal expectations in terms of quality of cartilage regeneration. However, this study has been necessary to demonstrate the feasibility of such innovative technique and, also, the applicability of live 3D printing for cartilage regeneration in a pre-clinical setting. Another important limitation of this study

Author Manuscript

This article is protected by copyright. All rights reserved.

is the difficulty in detecting whether the bioscaffold has remained in situ or not. In some cases, the macroscopic and microscopic appearances of the HH and BB groups were similar to the negative control group. This indicates that the scaffold may have moved from its original position. Based on previous literature (Deponti et al., 2014, Vinatier et al., 2009), we used fibrin glue in a spray form to try to avoid this complication, however we have found that its success could not be confirmed. We are currently undertaking in vitro studies with fluorescent labelling of cells and biomaterial, to investigate this issue. We are working on a chemical modification of the biomaterial that would allow its immediate adhesion to the host tissue, making the fibrin glue redundant by guaranteeing the immediate graft-host adhesion. Another limitation is due to the limited comparability of BB and HH Bioscaffolds: The BB group, in fact, was constituted by a biomaterial that, despite having the same backbone of the HH group (HA-GelMa), was printed in a non-coaxial way and subsequently embedded with cells. This was chosen to recapitulate the current methodology of cellularized scaffolds used for cartilage regeneration. We acknowledge that the lack of co-axial distribution, which is used to promote cell survival in the in-situ 3D bioprinting and therefore was not necessary in the BB technique, might make the BB scaffold not perfectly comparable with the HH scaffold. Finally, this study evaluates the early cartilage regeneration in a purely chondral defect. In the vast majority of the clinical cases, the subchondral bone is involved as well and needs to be reconstructed or, at least, supported. One of the major advantages of the Biopen

Author Manuscript

This article is protected by copyright. All rights reserved.

is the possibility to 3D print in "real-time" multiple layers using different biomaterials and/or cells to reconstitute different tissues, simply by changing cartridges. We have started with cartilage only defects to limit confounding factors and to simplify the approach, keeping in mind this is a pilot study. The next step of this approach would be to add one more tissue to regenerate (bone) and to use a different bioink for bone in a gradient fashion.

Conclusion

This pilot study shows that real-time intra-operative 3D bioprinting is feasible and can be done for the repair and regeneration of cartilage defects. We demonstrated both safety and the early promise of clinical efficacy.

The regenerated cartilage at early time points showed better overall macroscopic and microscopic characteristics when compared to pre-constructed 3D Bioscaffolds, microfractures and untreated controls. Studies with a longer follow up are now necessary to assess the quality of the cartilage regeneration in the long term.

To our knowledge, this is the first in vivo study of "live" in situ 3D bio-printing. This technology could potentially revolutionize the use of 3D printing techniques in tissue engineering, not only for musculoskeletal conditions, but also for other tissue or organ regeneration.

Author Manuscript

This article is protected by copyright. All rights reserved.

Author Manuscript

This article is protected by copyright. All rights reserved.

Acknowledgements

We would like to thank Dr Ken Ye and Dr Bill Zhang for providing the blinded macroscopic cartilage scoring of the specimens; Ms Danielle Baldwin for her assistance during cartilage specimen retrieval; Mr Pierre-Adrien Buisson for his help in the post-processing of the biomechanical data and Dr Tim Spelman for the statistical analysis.

This study has been partially funded by Arthritis Australia – Zimmer Australia grant, and by the Research Endowment Funds – St Vincent's Hospital, Melbourne.

Funding from the Australian Research Council Centre of Excellence Scheme (Project Number CE 140100012) is gratefully acknowledged. GGW is grateful to the ARC for support under the Australian Laureate Fellowship scheme (FL110100196). The authors also gratefully acknowledge the use of facilities within the Australian National Fabrication Facility (ANFF).

Author Manuscript

This article is protected by copyright. All rights reserved.

REFERENCES

BALINT, L., PARK, S. H., BELLYEI, A., LUCK, J. V., JR., SARMIENTO, A. & LOVASZ, G. 2005. Repair of steps and gaps in articular fracture models. *Clin Orthop Relat Res*, 208-18.

BRITTBERG, M. & WINALSKI, C. S. 2003. Evaluation of cartilage injuries and repair. *J Bone Joint Surg Am,* 85-A Suppl 2, 58-69.

DEPONTI, D., DI GIANCAMILLO, A., GERVASO, F., DOMENICUCCI, M., DOMENEGHINI, C., SANNINO, A. & PERETTI, G. M. 2014. Collagen scaffold for cartilage tissue engineering: the benefit of fibrin glue and the proper culture time in an infant cartilage model. *Tissue Eng Part A,* 20, 1113-26.

FEDOROVICH, N. E., SCHUURMAN, W., WIJNBERG, H. M., PRINS, H. J., VAN WEEREN, P. R., MALDA, J., ALBLAS, J. & DHERT, W. J. 2012. Biofabrication of osteochondral tissue equivalents by printing topologically defined, cell-laden hydrogel scaffolds. *Tissue Eng Part C Methods,* 18, 33-44.

HUNZIKER, E. B. 2002. Articular cartilage repair: basic science and clinical progress. A review of the current status and prospects. *Osteoarthritis Cartilage,* 10, 432-63.

JAKOB, R. P., FRANZ, T., GAUTIER, E. & MAINIL-VARLET, P. 2002. Autologous osteochondral grafting in the knee: indication, results, and reflections. *Clin Orthop Relat Res*, 170-84.

JEONG, C. G. & ATALA, A. 2015. 3D Printing and Biofabrication for Load Bearing Tissue Engineering. *Adv Exp Med Biol,* 881, 3-14.

KHAN, I. M., GILBERT, S. J., SINGHRAO, S. K., DUANCE, V. C. & ARCHER, C. W. 2008. Cartilage integration: evaluation of the reasons for failure of integration during cartilage repair. A review. *Eur Cell Mater,* 16, 26-39.

KORHONEN, R. K., LAASANEN, M. S., TOYRAS, J., RIEPPO, J., HIRVONEN, J., HELMINEN, H. J. & JURVELIN, J. S. 2002. Comparison of the equilibrium response of articular cartilage in unconfined compression, confined compression and indentation. *J Biomech,* 35, 903-9.

O'CONNELL, C. D. B., C; THOMPSON, F; AUGUSTINE, C; BEIRNE, S; CORNOCK, R; RICHARDS, C; CHUNG, J; GAMBHIR, S; YUE, Z; BOURKE, J; ZHANG, B; TAYLOR, A; QUIGLEY, A; KAPSA, R; CHOONG, P; WALLACE, G 2016. Development of the Biopen: A handheld device for surgical printing of adipose stem cells at a chondral wound site. *Biofabrication*.

RUTGERS, M., VAN PELT, M. J., DHERT, W. J., CREEMERS, L. B. & SARIS, D. B. 2010. Evaluation of histological scoring systems for tissue-engineered, repaired and osteoarthritic cartilage. *Osteoarthritis Cartilage,* 18, 12-23.

SCHUURMAN, W., LEVETT, P. A., POT, M. W., VAN WEEREN, P. R., DHERT, W. J., HUTMACHER, D. W., MELCHELS, F. P., KLEIN, T. J. & MALDA, J. 2013. Gelatin-methacrylamide hydrogels as potential biomaterials for fabrication of tissue-engineered cartilage constructs. *Macromol Biosci,* 13, 551-61.

Author Manuscript

This article is protected by copyright. All rights reserved.

SHARMA, B., FERMANIAN, S., GIBSON, M., UNTERMAN, S., HERZKA, D. A., CASCIO, B., COBURN, J., HUI, A. Y., MARCUS, N., GOLD, G. E. & ELISSEEFF, J. H. 2013. Human cartilage repair with a photoreactive adhesive-hydrogel composite. *Sci Transl Med,* 5**,** 167ra6.

STOK, K. S., LISIGNOLI, G., CRISTINO, S., FACCHINI, A. & MULLER, R. 2010. Mechano-functional assessment of human mesenchymal stem cells grown in three-dimensional hyaluronan-based scaffolds for cartilage tissue engineering. *J Biomed Mater Res A,* 93**,** 37-45.

TOGNANA, E., CHEN, F., PADERA, R. F., LEDDY, H. A., CHRISTENSEN, S. E., GUILAK, F., VUNJAK-NOVAKOVIC, G. & FREED, L. E. 2005. Adjacent tissues (cartilage, bone) affect the functional integration of engineered calf cartilage in vitro. *Osteoarthritis Cartilage,* 13**,** 129-38.

VAN DEN BORNE, M. P., RAIJMAKERS, N. J., VANLAUWE, J., VICTOR, J., DE JONG, S. N., BELLEMANS, J., SARIS, D. B. & INTERNATIONAL CARTILAGE REPAIR, S. 2007. International Cartilage Repair Society (ICRS) and Oswestry macroscopic cartilage evaluation scores validated for use in Autologous Chondrocyte Implantation (ACI) and microfracture. *Osteoarthritis Cartilage,* 15**,** 1397-402.

VINATIER, C., GAUTHIER, O., MASSON, M., MALARD, O., MOREAU, A., FELLAH, B. H., BILBAN, M., SPAETHE, R., DACULSI, G. & GUICHEUX, J. 2009. Nasal chondrocytes and fibrin sealant for cartilage tissue engineering. *J Biomed Mater Res A,* 89**,** 176-85.

YE, K., FELIMBAN, R., TRAIANEDES, K., MOULTON, S. E., WALLACE, G. G., CHUNG, J., QUIGLEY, A., CHOONG, P. F. & MYERS, D. E. 2014. Chondrogenesis of infrapatellar fat pad derived adipose stem cells in 3D printed chitosan scaffold. *PLoS One,* 9**,** e99410.

Author Manuscript

This article is protected by copyright. All rights reserved.

AUTHORS CONTRIBUTION STATEMENT

- **Claudia Di Bella**. Principal contributor. Conception and design of the project, obtaining funds, performance of animal surgery, analysis and interpretation of data, writing of the manuscript and final approval of the article.
- **Serena Duchi**. Conception and design of biochemical tests (histology and immunohistochemistry), analysis and interpretation of the data, drafting of the pictures, critical revision of the manuscript.
- **Cathal D. O'Connell**. Contributions to the design of the hydrogel 'bioink' composition; contributions to design of procedures for biopen printing, including cell encapsulation protocols, materials preparation protocols and photocuring protocols; analysis and interpretation of data regarding material properties and the biopen printing performance. Critical revision of the manuscript.
- **Romane Blanchard**. Development of the design of the biomechanical indentation protocol, performance of the biomechanical tests and analysis of the biomechanical data.
- **Cheryl Augustine**. Administrative and technical support for the preparation of cellular components of the biomaterial and technical support during the surgical procedures. Collection and assembly of the data.
- **Zhilian Yue**. Establishment of the protocol for material synthesis and formulation including crosslinking conditions, critical revision of manuscript.
- **Fletcher Thompson**. Bioengineer directly involved in the development and optimisation of the Biopen for surgical application. Technical support during surgical procedure.
- **Christopeh Richards**. Optimisation of the geometry (CAD modelling of 3D structures, characterisation of the extrusion profile, degree of infill) and associated printing parameters (pressure, head temperature, base temperature, speed) of GelMA scaffolds. Overview and technical input regarding machine operation for procedures and standard protocols used in the production of scaffolds.
- **Stephen Beirne**. Design and development of the biopen since its very inception.
- **Carmine Onofrillo**. Technical support on production of biochemical data and performance of biochemical tests, analysis and interpretation of data.
- **Sebastien H. Bauquier**. Establishment and improvement of the anaesthetic and analgesic protocols used in the animal surgery, contribution in gaining the Animal Ethic approval. Performance of post-operative assessment of the animals. Critical revision of the manuscript

Author Manuscript

This article is protected by copyright. All rights reserved.

- **Stewart D. Ryan**. Development of the study design for the large animal component of the study, arranging sourcing and housing of the animals, submission of Animal Ethics application and subsequent revision and extra monitoring of animals. Performance of animal surgery. Critical revision of the manuscript.
- **Peter Pivonka**. Oversight and intellectual input in concept and design of biomechanical tests and analysis of biomechanical data. Draft of the biomechanical section of the manuscript and critical revision of the final manuscript.
- **Prof Gordon G. Wallace**. Director of ACES – University of Wollongong. Funds obtainment. Overall supervision of all the bioengineering and biomaterial components of the project. Critical revision of manuscript.
- **Prof Peter F. Choong**. Director of Department of Surgery – University of Melbourne. Finds obtainment. Overall supervision of the entire project. Critical revision of manuscript.

Author Manuscript

This article is protected by copyright. All rights reserved.

ICRS Macroscopic Scoring	Points
Degree of defect repair	
In level with surrounding cartilage	4
75% depth of defect repair	3
50% depth of defect repair	2
25% depth of defect repair	1
0% depth of defect repair	0
Integration to border zone	
Complete integration	4
Demarcating border < 1mm	3
¾ of graft integrated (border >1 mm in ¼)	2
½ of graft integrated (border > 1mm in ½)	1
¼ of graft integrated, or no integration	0
Macroscopic appearance	
Intact smooth surface	4
Fibrillated surface	3
Small, scattered fissures or cracs	2
Several, small or few but large fissures	1
Total degeneration of grafted area	0

Table 1.

Author Manuscript

This article is protected by copyright. All rights reserved.

O'Driscoll Modified Histology Scoring	Points
Tissue morphology	
Exclusively non cartilage	1
Mostly non cartilage	2
Mostly fibrocartilage	3
Mostly hyaline cartilage	4
Matrix staining	
None	1
Slight	2
Moderate	3
Strong	4
Structural integrity	
Severe disintegration	1
Cysts or disruption	2
No organization of chondrocytes	3
Beginning of columnar organization of chondrocytes	4
Normal, similar to healthy mature cartilage	5
Chondrocyte clustering in implant	
25-100% cells clustered	1
<25% cells clustered	2
No clusters	3
Intactness of calcified layer/tidemark	
<25% intact	1
25-49% intact	2
50-75% intact	3
76-90% intact	4
Completely intact	5
Subchondral bone formation	
No formation/collapse	1
Slight	2
Strong	3
Histological appraisal of surface architecture	
Severe fibrillation or disruption	1
Moderate fibrillation or irregularity	2
Slight fibrillation or irregularity	3
Normal	4
Histological appraisal of defect filling	
<25%	1
26-50%	2
51-75%	3
76-90%	4
91-110%	5
Lateral integration of implanted material	
Not bonded	1
Bonded at one end only/partially at both ends	2
Fully bonded at both ends	3
Basal integration of implanted material	
<50%	1
51-75%	2
76-90%	3
91-100%	4

This article is protected by copyright. All rights reserved.

Inflammation	
Strong inflammation	1
Slight inflammation	3
No inflammation	5
TOTAL MAXIMUM SCORE AVAILABLE	**45**

Table 2.
Table Legend.

Table 1. Macroscopic scoring system according to ICRS (van den Borne et al., 2007). The overall repair assessment is graded as: Grade I (normal)= score 12; Grade II (nearly normal)= score 11-8; Grade III (abnormal)= 7-4; Grade IV (severely abnormal) = 3-0.

Table 2. Modified O'Driscoll histological score

Figure Legend

Fig 1. (a) Design of the Biopen, which shows the two separate chambers with a motor control. The two chambers are connected to the printing nozzle (Insert), which allows the co-axial printing of the two different bioink in a core/shell distribution. (b) Photograph of the Biopen. (c) Representation of the core/shell distribution. The HA-GelMa in the shell includes the photoinitiator VA-086 for UV photocuring, which gives mechanical support to the printed biomaterial and, at the same time, protects the inner core. The HA-GelMa in the core does not

Author Manuscript

This article is protected by copyright. All rights reserved.

contain photoinitiator, but includes MSCs. (d) Representation of the multiple layers 3D printed block in a criss-cross pattern.

Fig 2. A full thickness chondral defect has been performed in the weight bearing area of the medial and lateral femoral condyles of both stifle joints (a). (b) Intra-operative photographs of the Biopen in action. (c) Defect filled with HH Bioscaffold and coated with fibrin glue spray. The circular defect is visible, and it is macroscopically fully filled maintaining the apparent curvature of the femoral condyle. (d) Macroscopic picture of the retrieved specimen: an osteochondral block centred over the defect is removed, and bisected to allow biomechanical and biochemical tests.

Fig 3. (a) Macroscopic appearance of the defects at explant. (b) Box and whiskers plot of ICRS Macroscopic score by treatment group (n=6 per group). Macroscopic score shows large variation within each group, but overall is significantly better for the HH group compared to BB and MF group, and very close to significance (p=0.057) compared to C group. HH= Hand held Biopen printed scaffold; BB= Bench Based 3D printed scaffold; MF= Microfractures; C= Negative Control (defect left empty).

Fig 4. (a) Histology and Immunohistochemistry show better new cartilage formation in the HH group compared to the other groups. Subchondral cysts and

This article is protected by copyright. All rights reserved.

collapse are seen in the BB and MF group, with fibrocartilage formation. Minimal new cartilage formation is seen in the Control Group. Maintenance of the subchondral bone, calcified cartilage layer and cartilage height is seen in the HH group, with occasional evidence of columnar chondrocyte distribution. (b) Box and whiskers plot of modified O'Driscoll score. Statistically significant improved cartilage formation is seen in the HH group compared to the MF group.
HH= Hand held Biopen printed scaffold; BB= Bench Based 3D printed scaffold; MF= Microfractures; C= Negative Control (defect left empty).

Fig 5. (a) Indentation of the half condyle specimen in PBS solution; results obtained from mechanical testing for each group show: (b) thickness; (c) instantaneous Young's modulus (t=0); (d) equilibrium modulus and (e) maximum stress.

Author Manuscript

This article is protected by copyright. All rights reserved.

Author Manuscript

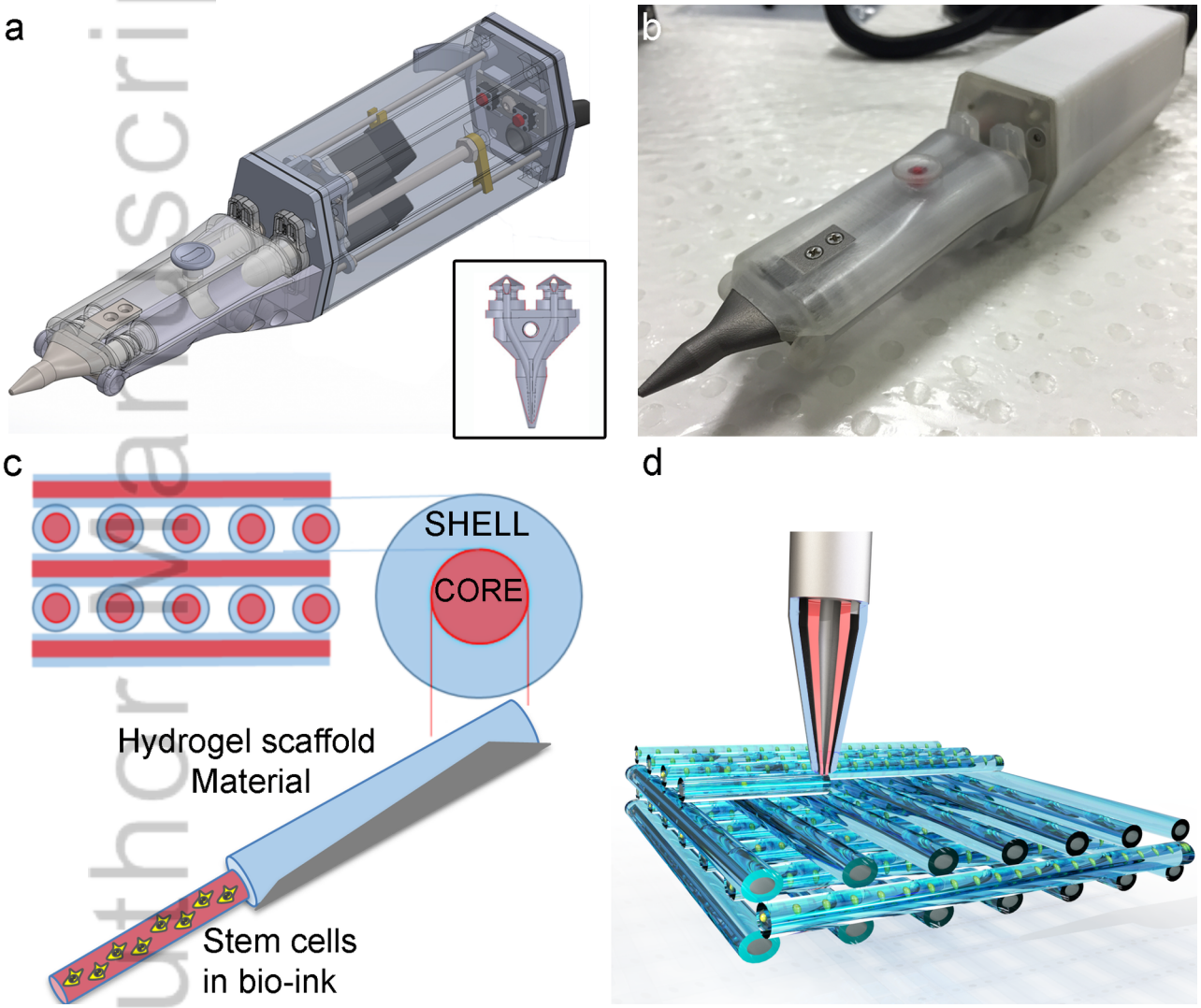

TERM_2476_F1.tif

This article is protected by copyright. All rights reserved.

Author Manuscript

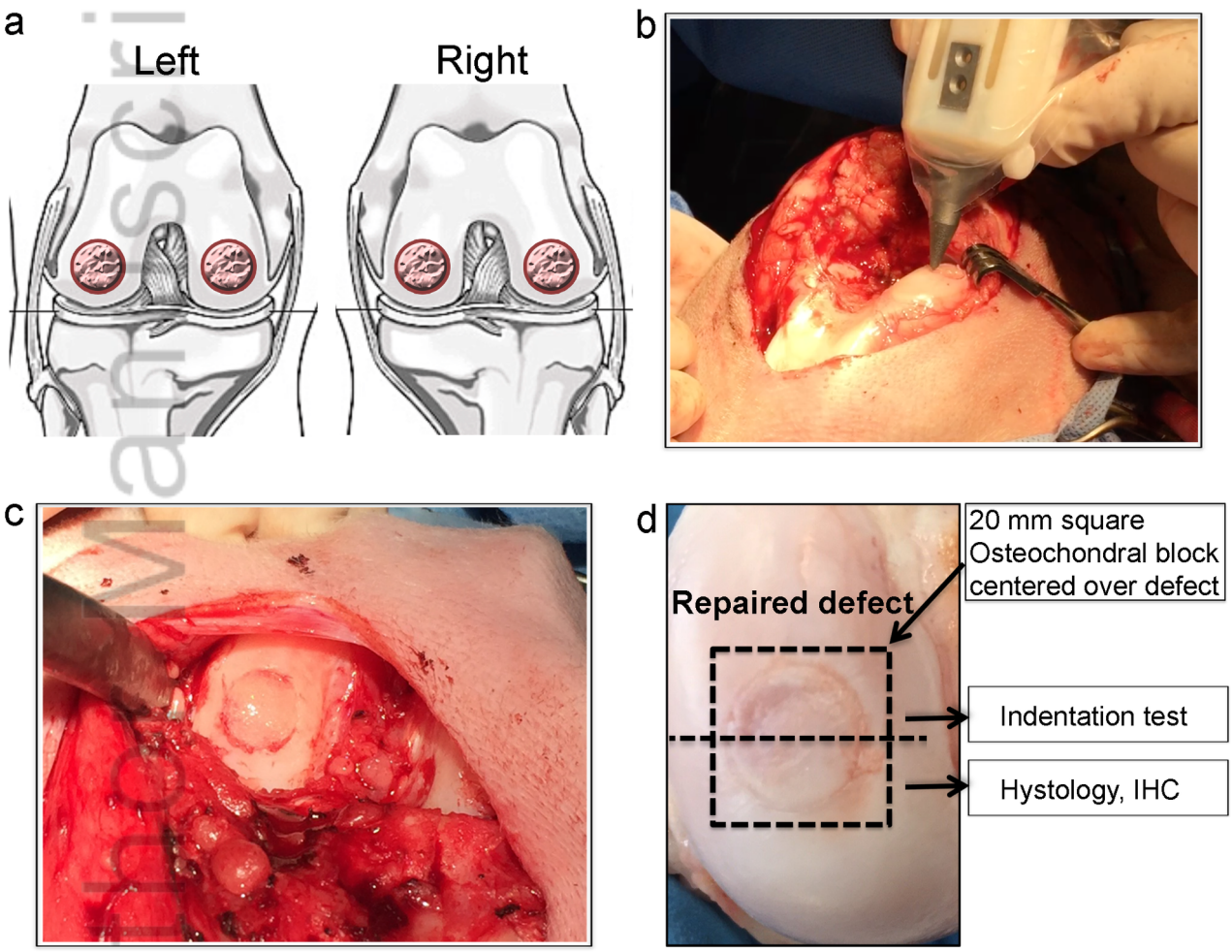

TERM_2476_F2.tif

This article is protected by copyright. All rights reserved.

Author Manuscript

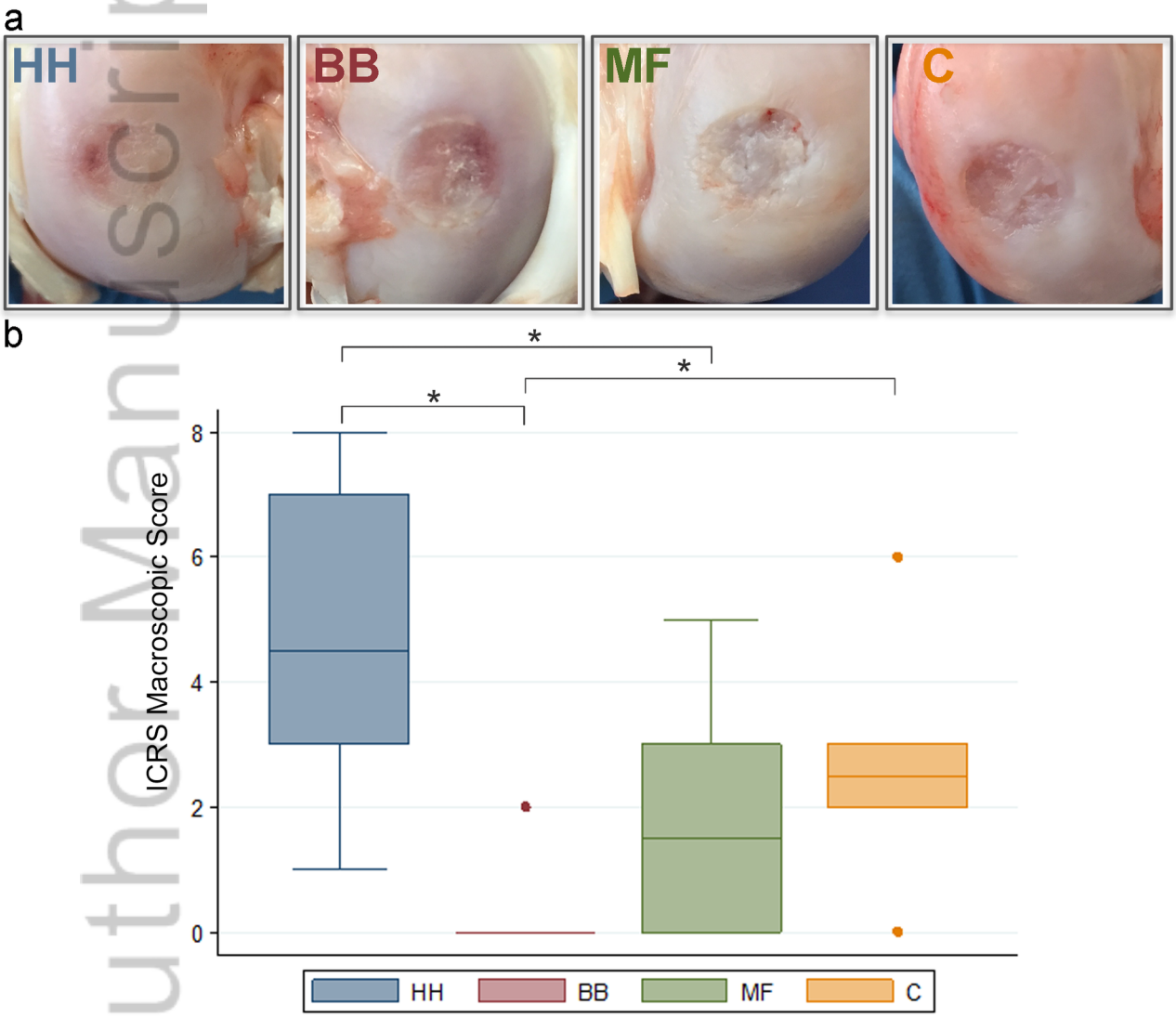

TERM_2476_F3.tif

This article is protected by copyright. All rights reserved.

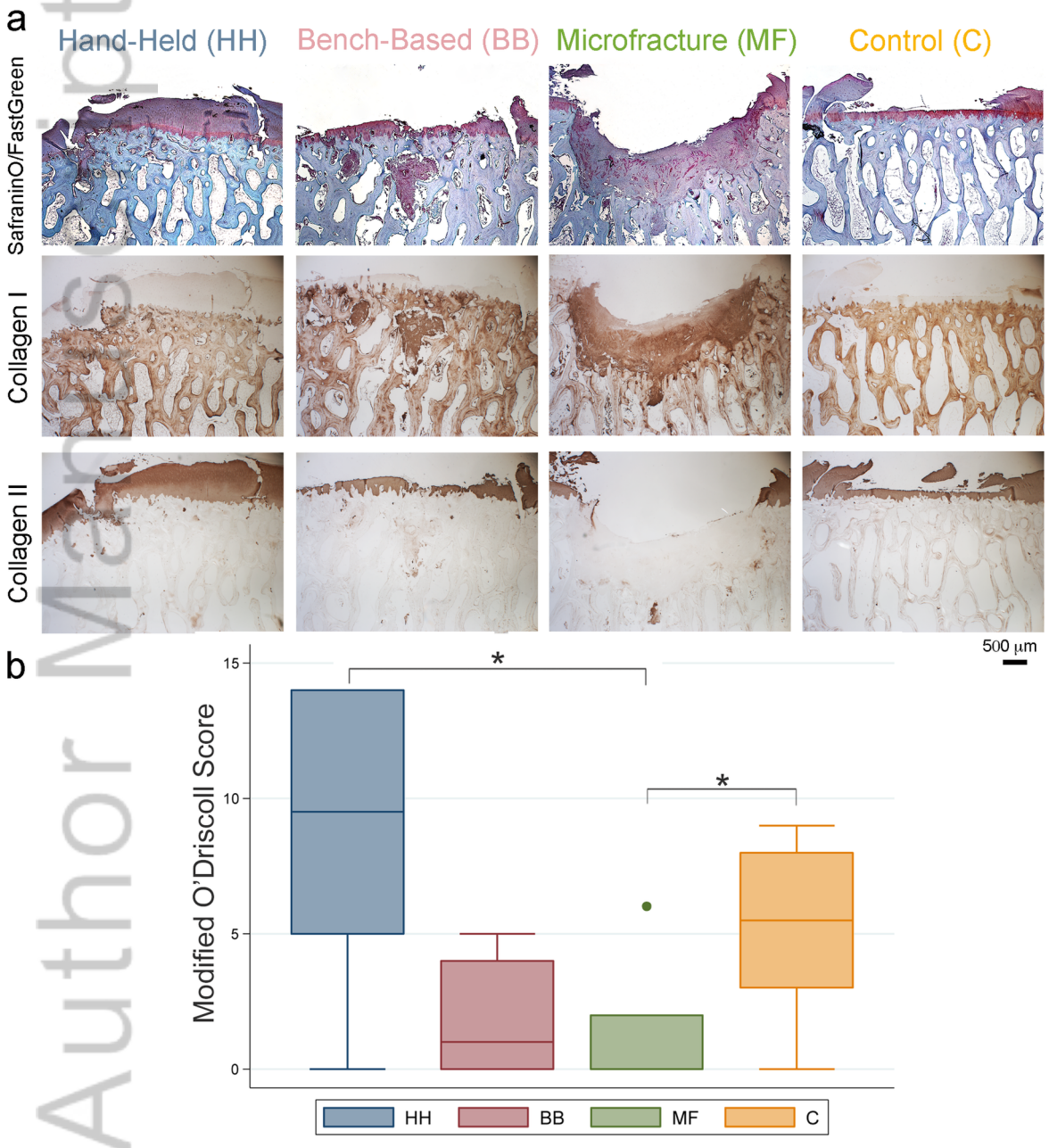

TERM_2476_F4.tif

Author Manuscript

This article is protected by copyright. All rights reserved.

Author Manuscript

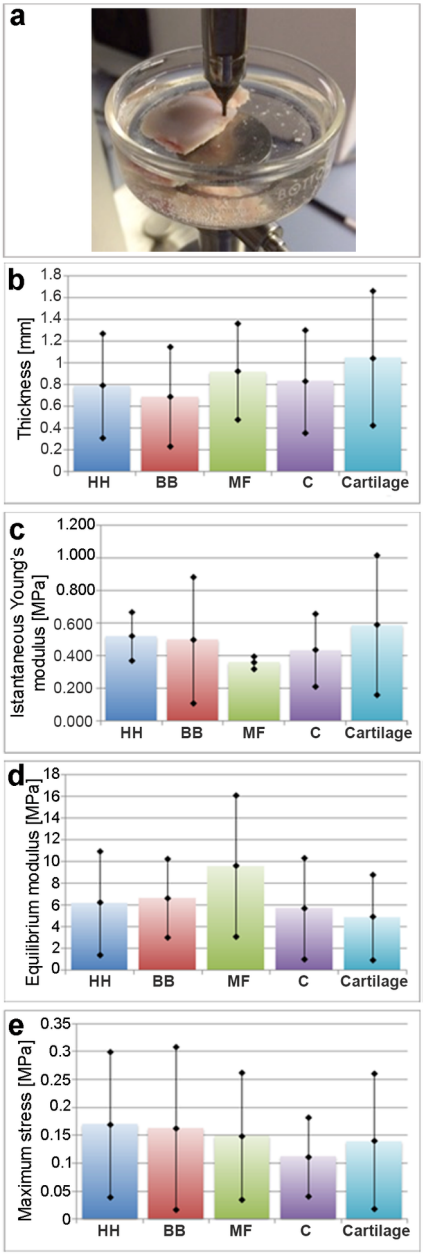

TERM_2476_F5.tif

This article is protected by copyright. All rights reserved.